



Modeling intra-particle convection in heterogeneous non-catalytic reacting systems

Natércia C. P. Fernandes*, José A. A. M. Castro

Department of Chemical Engineering, University of Coimbra, Pólo II, Pinhal de Marrocos, 3030-290 Coimbra, Portugal

Received 27 July 2001; received in revised form 16 April 2002; accepted 16 May 2002

Abstract

A dynamic mechanistic model of a multi-phase heterogeneous batch reactor processing a non-catalytic fluid–solid reaction is developed and numerically solved. The model takes into account both intra-particle convection and diffusion phenomena, as well as chemical reaction between the fluid and the solid. By addressing the until now ignored case of convection originated by the continuous increase of the particle porosity, this work enables a more realistic modeling of many non-catalytic fluid–solid reaction systems. The dependency of the convective term on the chemical reaction rates gives rise to a space and time dependency of the intra-particle velocity thus increasing the mathematical complexity of the problem. The model is characterized by a set of PDEs coupled with adequate boundary conditions that are solved by the method of lines. An example of application of great importance to the chemical pulping of wood is used, emphasizing the differences with the typical situation where only diffusion is considered.

© 2002 Elsevier Science Ltd. All rights reserved.

Keywords: Simulation; Mathematical modeling; Multi-phase reactor; Intra-particle convection; Variable porosity; Pulping digester

1. Introduction

In the task of modeling a fixed bed reactor whose operation is governed by pore diffusion limitations it is mandatory to consider the intra-particle diffusion that is often represented by the so-called “Fick’s law”. However, some authors have claimed that, in certain circumstances, diffusion is not the only transport mechanism that should be considered in the analysis of fluid–solid reaction systems. One of the earlier efforts was that of [Aris and Kehoe \(1973\)](#) who studied the effect of the volume change caused by a simple reaction on the catalyst internal pressure, having concluded that the pressure gradients do not contribute significantly to the overall flux in the pores and can be discarded in the analysis of this specific situation. [Komiya and Inoue \(1974\)](#) have shown for the first time that intra-particle convection is a transport phenomenon which cannot be neglected in large pore catalysts. Since the particles packed in a fixed bed reactor are exposed to a longitudinal pressure gradient resulting mainly from flow resistances, there is a flow through the catalyst pores. Obviously, the larger the pores, the

more significant is the convection relatively to the diffusion. These authors proposed a theoretical model accounting for the referred convective term. They computed the pressure drop in the packed bed using the Kozeny–Carmen relationship and, assuming that the pressure varies linearly along the reactor bed length, found the pressure drop between the top and the bottom of a single particle. From Darcy’s law and the assumption that the small pressure drop between the top and the bottom of the particle is time and space invariant they reached a constant value for the intra-particle velocity.

Another pioneer work is due to [Pismen \(1976\)](#) in studying the counter-current gas and liquid flows induced by chemical reaction inside a partially liquid-filled porous body. The reaction and the transfer process itself give rise to composition profiles across the particle. The liquid becomes unequally volatile and, therefore, the vapor moves from high to low volatile regions. After condensation in these low volatile domains, capillary forces direct the liquid back.

[Nir and Pismen \(1977\)](#) also studied the effect of forced intra-particle convection in catalytic systems but their modeling strategy was similar to that of [Komiya and Inoue \(1974\)](#), described above. An extension of this strategy was developed by [Ferreira \(1988\)](#) to consider the more realistic situations of non-isothermal catalyst particles.

* Corresponding author. Tel.: +351-239-798-700;
fax: +351-239-798-703.

E-mail address: natercia@eq.uc.pt (N. C. P. Fernandes).

Since then much research work concerning this subject has been carried out, mainly by Rodrigues and co-workers. Lopes, Dias, Mata, and Rodrigues (1995) studied the non-isothermal effects on the efficiency of large-pore particles with slab and sphere geometries. Simultaneously, Sun, Costa, and Rodrigues (1995) experimentally determined the effective diffusivities and convective coefficients of pure gases in single pellets. Later, Nan, Dias, Lopes, and Rodrigues (1996) developed an analogy between slab and cylinder geometries when diffusion, forced convection and reaction inside the catalyst should be considered and presented an analytical steady-state solution. Another important contribution is due to Pfeiffer, Chen, and Hsu (1996), who measured the volumetric flow rate of liquid and gas through very small gigaporous particles, obtaining values 4–17 times greater than those calculated using variations of the Carmen–Kozeny equation. More recently, Ferreira, Costa, and Rodrigues (1996) analyzed the effect of convective flow inside large-pore slab catalysts on the transient behavior of fixed-bed reactors. At the same time, Leitão and Rodrigues (1996) took into account the convective flow in modeling the biodegradation/adsorption combined process in fixed-bed biofilm reactors. It is noteworthy that in all these studies the underlying reason for the existence of intra-particle convection is a pressure drop between the top and the bottom of the particle. The usual practice is to compute the overall pressure drop along the reactor through empirical equations and to use this value to estimate the pressure drop for a single particle. With this value, a constant intra-particle velocity is finally computed.

In this work one addresses a different problem involving intra-particle convection that has not been studied before. In the present situation the convective term is not caused by a constant pressure drop between the extremes of the particle but instead is the complex result of cumulative porosity changes since the center until a given point of the particle due to a non-catalytic fluid–solid chemical reaction. There is no pressure driving force for flow in the porous media. The convection is caused entirely by the flow of liquid which fills up the pores caused by reaction. A dynamic mechanistic model (describing the most important multi-phase reactor in the pulp and paper industry) which takes into account simultaneous reaction, intra-particle diffusion and convection is developed and numerically solved. An algorithm to compute the coefficients of this model, namely the intra-particle velocity profile generated by the chemical reaction, is presented. This space varying particle porosity represents a seldom studied situation that induces itself a space varying intra-particle convection.

2. Modeling

The uncommon features of the kraft pulping process make the modeling of this highly heterogeneous system especially

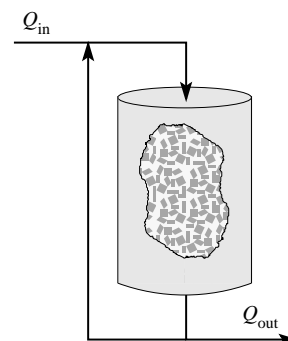


Fig. 1. Simplified schematic representation of the reactor.

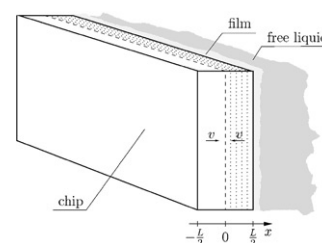


Fig. 2. Representation of a chip.

appealing not only from a practical but also from a scientific point of view. Essentially, the reactor is a “cylinder” filled up with a bed of porous wood particles immersed in a solution where several inorganic chemicals are dissolved (see Fig. 1), namely sodium hydroxide and sodium sulfide.

The particles are wood chips, whose pores are completely impregnated with “entrapped liquid”. One of these particles is schematically detailed in Fig. 2.

It is inside the chip pores that the reactions between the inorganic chemicals dissolved in the entrapped liquid and the organic compounds of the solid matrix of wood take place. The surrounding solution, called “free liquid”, recirculates through the reactor, leading to a homogeneous distribution of all dissolved substances along the reactor volume. These substances are organic and inorganic compounds (reaction products and reactants, respectively). The concentrations of both reactants and reaction products inside the particles depend on the rates of the transport mechanisms across the chip and of the fluid–solid chemical reactions. The most significant of these mechanisms is undoubtedly the diffusion, that is responsible for the motion of reactants from the chip edge to the chip center and of reaction products in the opposite direction. However, it is not the only phenomenon involved. As referred above, the solid matrix of the particles provides, itself, some of the reactant material for the

chemical reaction. Therefore, part of the solid phase is consumed as the reaction proceeds making the particles more and more porous. This increase in porosity occurs inwards, i.e., from the particle surface to its center replicating the behavior of the chemical reaction. The inorganic reactants, initially dissolved in the free liquid, move into the wood chips due to two distinct reasons: on one hand, because their concentration is higher in the free phase than in the entrapped one and, on the other, because the increase of the particle voidage generates a flow from the surrounding liquid into the chip. There is experimental evidence that the mass transport by convection can be up to 10% of the overall transport (Costa, Francisco, Simo, Egas, and Castro, 2001) showing that it might play a significant role on the reactor behavior.

Based on this general description, a mechanistic model of the system can be developed.

2.1. Mass balances

A global mass balance for the free liquid in the reactor, together with the assumption of constant liquid density, leads to

$$\frac{dV_f}{dt} = Q_{in} - Q_{out} - Q_{fe}, \quad (1)$$

where Q_{fe} is the volumetric flow rate of free liquid moving by convection into the particles. A partial mass balance for a generic species k in the free liquid gives

$$\begin{aligned} \frac{d}{dt} (C_{f,k} V_f) &= C_{in,k} Q_{in} - C_{f,k} (Q_{out} + Q_{fe}) \\ &+ K_k a_{fe} (C_{e,k}|_{x=L/2} - C_{f,k}), \end{aligned} \quad (2)$$

where $C_{p,k}$ denotes the concentration of the species k in the phase or flow p and L is the particle thickness. Coupling Eq. (1) with Eq. (2) it is possible to reach

$$\frac{dC_{f,k}}{dt} = \frac{Q_{in}(C_{in,k} - C_{f,k}) + K_k a_{fe}(C_{e,k}|_{x=L/2} - C_{f,k})}{V_f}. \quad (3)$$

As the reaction proceeds, the volume of free liquid, V_f , decreases with time, while the effective inter-facial area between the free and entrapped liquids, a_{fe} , increases due to the increase in porosity.

To determine the time evolution of the concentration of a generic substance k dissolved in the entrapped liquid phase inside the particle, a partial microscopic mass balance is used

$$\frac{\partial}{\partial t} (\varepsilon_c C_{e,k}) = \frac{\partial}{\partial x} \left(\mathcal{D}_k \frac{\partial C_{e,k}}{\partial x} \right) - \frac{\partial}{\partial x} (\varepsilon_c v C_{e,k}) + \alpha_k |\mathcal{R}_k| \quad (4)$$

with

$$\alpha_k = \begin{cases} -\varepsilon_c & \text{if } k \text{ is inorganic,} \\ \rho_{c,OD} & \text{if } k \text{ is organic.} \end{cases} \quad (5)$$

Eq. (4) can be rearranged into

$$\begin{aligned} \frac{\partial C_{e,k}}{\partial t} &= \frac{1}{\varepsilon_c} \left(-\frac{\partial \varepsilon_c}{\partial t} C_{e,k} + \frac{\partial \mathcal{D}_k}{\partial x} \frac{\partial C_{e,k}}{\partial x} + \mathcal{D}_k \frac{\partial^2 C_{e,k}}{\partial x^2} \right. \\ &\left. - \frac{\partial}{\partial x} (\varepsilon_c v C_{e,k}) + \alpha_k |\mathcal{R}_k| \right). \end{aligned} \quad (6)$$

It should be noted that the parameters chip porosity, ε_c , diffusion coefficient, \mathcal{D}_k , and intra-particle velocity, v , do vary with both time and spatial coordinate of the solid particle.

The mass fractions of the organic components of the solid phase, $C_{s,k}$, based on the initial oven dry wood, depend only on the rates of reaction with the inorganic chemicals and are described by equations of the form

$$\frac{\partial C_{s,k}}{\partial t} = -|\mathcal{R}_k|. \quad (7)$$

Eqs. (1), (3), (6), and (7) form the basis of the proposed model.

2.2. Model coefficients

Particle voidage: Since the porosity of the particle depends on the extent of reaction, it is a function of both time and space. The porosity at a generic point inside the chip can be computed by (Fernandes & Castro, 2000).

$$\varepsilon_c(x, t) = 1 - (1 - \varepsilon_{c,i}) \eta(x, t), \quad (8)$$

where $\varepsilon_{c,i}$ is the initial average porosity of the chips and the yield $\eta(x, t)$ is the sum of the local mass fractions of all organic compounds in the solid matrix and is given by

$$\eta(x, t) = \sum_{k=1}^{n_o} C_{s,k}(x, t). \quad (9)$$

Porosity change: The model also requires the partial derivative of porosity with time. From Eq. (8) and heeding to Eqs. (7) and (9) it is possible to reach, after simplification

$$\frac{\partial \varepsilon_c}{\partial t} = (1 - \varepsilon_{c,i}) \sum_{k=1}^{n_o} |\mathcal{R}_k|. \quad (10)$$

Interface area: According to Dupuit's law it is possible to prove that, for a random distribution of pores, the

ratio between the porous cross-sectional area and the total cross-sectional area is the same as the ratio between the porous volume and the total volume, i.e., the porosity (Froment & Bishoff, 1990). Therefore,

$$a_e(x, t) = \varepsilon_c(x, t)a_c, \quad (11)$$

where the porosity is given by Eq. (8) and both a_e and a_c refer to the total number of particles in the reactor rather than to a single chip. The area of interface between the free and entrapped liquids is the effective capillary cross-sectional area at the chip edge ($x = L/2$):

$$a_{fe} = \varepsilon_c|_{x=L/2}a_c. \quad (12)$$

Intra-particle velocity: Since the intra-particle convection is originated by the change of porosity and not by a forced motion of the free liquid through the chip, the “flow” of liquid across the slab decreases from the chip edge to the chip center (where it is zero). As it has been already mentioned above, this leads to symmetric velocity profiles relatively to the chip center. The velocity of the fluid at a given point inside the chip can be computed from

$$v(x, t) = \frac{Q(x, t)}{a_e(x, t)}. \quad (13)$$

The liquid flow at a generic point x_j of the x -axis (spatial coordinate along the chip thickness) represents all the liquid needed to fill up the new inner volume generated by the chemical dissolution of the solid matrix between $x = 0$ (chip center) and the point x_j . Thus, the convective liquid flow at a generic position x_j inside the chip is given by

$$Q(x_j, t) = -\frac{\partial}{\partial t} \left(\int_0^{x_j} \varepsilon_c(x, t)a_c dx \right). \quad (14)$$

Substituting Eqs. (11) and (14) into Eq. (13) it is possible to obtain, after simplification

$$v(x_j, t) = -\frac{1}{\varepsilon_c(x_j, t)} \int_0^{x_j} \frac{\partial \varepsilon_c(x, t)}{\partial t} dx, \quad (15)$$

where the partial derivative of the chip porosity with time is given by Eq. (10). This velocity depends on the reaction extent in two antagonistic ways:

- On one hand, if the chemical reaction rate increases the change in porosity will be faster, leading to an increase in the intra-particle velocity profile;
- On the other hand, as the reaction proceeds the porosity increases, thus increasing the porous cross-sectional area. This promotes a decrease in the intra-particle velocity.

Volume of free liquid: The total flow of fluid from the free liquid into the chip, Q_{fe} (Eq. (1)) is equal to the flow of liquid crossing the chip edge, $Q|_{x=L/2}$, i.e.,

$$Q_{fe} = |v|_{x=L/2}a_{fe}. \quad (16)$$

Thus, the final form of Eq. (1) is

$$\frac{dV_f}{dt} = Q_{in} - Q_{out} - |v|_{x=L/2}a_{fe}. \quad (17)$$

Effective diffusion coefficients: \mathcal{D}_k depends on the molecular diffusivity of species k and on the porosity and tortuosity of the solid matrix (Froment & Bishoff, 1990). In this work, the tortuosity is considered constant. Thus, the effective diffusion coefficient is updated with the porosity according to

$$\mathcal{D}_k(x, t) = \mathcal{D}'_{m,k} \varepsilon_c(x, t) \quad (18)$$

with the constant $\mathcal{D}'_{m,k}$ defined as

$$\mathcal{D}'_{m,k} = \frac{\mathcal{D}_{m,k}}{\tau}, \quad (19)$$

where $\mathcal{D}_{m,k}$ is the molecular diffusivity of species k .

2.3. Boundary conditions

To solve the set of PDEs defined by Eqs. (1), (3), (6), and (7) a consistent set of boundary conditions has to be selected and this should reflect the physical characteristics of the system:

- Both sides of the chip contact the free liquid, which means that they are exposed to the same external concentrations. Therefore, diffusion will induce symmetric profiles along the slab thickness.
- Since convection results from an increase in chip porosity due to chemical reaction and admitting that the initial conditions are the same along the chip thickness, the convective flows are symmetric relatively to the particle center.

Therefore, at the particle center ($x = 0$), for each species in phase p (either solid or entrapped liquid) one can consider that

$$\left. \frac{\partial C_{p,k}}{\partial x} \right|_{x=0} = 0. \quad (20)$$

The specifications at chip edge are the result of assuming equal mass fluxes at the chip surface ($x = L/2$):

$$\begin{aligned} a_c \mathcal{D}_k \left. \frac{\partial C_{e,k}}{\partial x} \right|_{x=L/2} + Q_{fe} C_{e,k}|_{x=L/2} \\ = K_k a_{fe} (C_{f,k} - C_{e,k}|_{x=L/2}) + Q_{fe} C_{f,k}. \end{aligned} \quad (21)$$

Attending to Eqs. (12) and (16) it is possible to transform Eq. (21) into

$$\begin{aligned} \left(\frac{\mathcal{D}_k}{\varepsilon_c} \frac{\partial C_{e,k}}{\partial x} \right) \Big|_{x=L/2} = (K_k - v|_{x=L/2}) \\ \times (C_{f,k} - C_{e,k}|_{x=L/2}). \end{aligned} \quad (22)$$

2.4. Numerical solution

The model equations are solved by the method of lines that transforms the problem into a system of ODEs. The partial differential equations were discretized using a constant step along the spatial coordinate of the particle, x , and the space derivatives were approximated by centered finite differences. The number of resulting ODEs, n_{eq} is

$$n_{\text{eq}} = n_f + (n + 1)(n_e + n_s), \quad (23)$$

where n_f , n_e , n_s and n designate the number of equations for the free liquid, for the entrapped liquid (at each chip position), for the solid phase (at each chip position) and the number of discretization intervals used between the chip center and the chip edge, respectively. The number of equations for each phase is given by

$$n_p = \begin{cases} n_i + n_o & \text{for free liquid,} \\ n_i + n_o & \text{for entrapped liquid,} \\ n_o & \text{for solid matrix.} \end{cases} \quad (24)$$

Due to limitations related to the adopted numerical approximation of the derivatives, the equations corresponding to the physical boundaries (chip center and chip edge) require the use of a fictitious point. The state variables corresponding to the solid and to the entrapped liquid in the particle can be computed at the fictitious point $j = -1$ using the discretized form of Eq. (20). In what concerns the fictitious point at $j = n + 1$, the state variables corresponding to the entrapped liquid can be computed from Eq. (22). However, for the variables characterizing the solid matrix a linear approximation was assumed in the vicinity of the chip edge, that is,

$$\frac{\partial^2 C_{s,k}}{\partial x^2} \Big|_{x=L/2} = 0. \quad (25)$$

Discretizing this equation it is then possible to estimate the required values for the solid phase variables at the fictitious point $j = n + 1$. It is worth mentioning the reason for the need of boundary conditions involving $C_{s,k}$. Both Eqs. (6) and (7) need $C_{s,k}$ for evaluation of \mathcal{R}_k . Additionally, Eq. (6) needs $C_{s,k}$ for evaluation of $\partial \varepsilon_c / \partial t$. Since Eq. (7) is an ODE one could think that no boundary conditions are needed. However, the requirement for boundary conditions involving $C_{s,k}$ comes from Eq. (6) and not from Eq. (7). The dependency of Eq. (6) on the solid state variables is not only the mentioned above. In fact, Eq. (6) contains v and ε_c in the argument of the spatial derivative. The variable v is a function of ε_c (see Eq. (15)), while ε_c is a function of $C_{s,k}$ (see Eqs. (8) and (9)), which makes Eq. (6) require boundary conditions involving the solid state variables.

The problem is numerically solved using the package DASPK, developed by Brown, Hindmarsh, and Petzold (1994, 1998). (see also Li & Petzold (1999)).

3. Discussion of results

A relevant application of the model developed here is in the chemical pulping of wood, a heterogeneous non-catalytic reaction process of utmost importance in the pulp and paper industry. A particular operational problem in this process is the non-uniformity of the final pulp that arises as a result of strong concentration gradients that are built up within the chip during the reactor operation. Therefore, the ability to predict such gradients is of great importance for the understanding and handling of the factors that affect this undesirable non-uniformity. In order to illustrate the model capabilities, the kinetic laws proposed by Mirams and Nguyen (1996) were used to compute the reaction rates of the organic species in the wood. It is noteworthy that this kinetic model was developed based on average solid matrix concentration measurements and on the concentrations of inorganic species in the free liquid. Since the work of Mirams and Nguyen (1996) does not include a law for the consumption rate of inorganic chemicals, the model employed by Fernandes and Castro (2000) was used after proper tuning with industrial data from a pulp mill. A “heterogeneous” kinetic model, based on concentrations inside the chip does not exist yet and, therefore, the model of Mirams and Nguyen (1996) is employed here for exemplifying purposes. Such approximation of using a “homogeneous” kinetic model to compute the reaction rates of a heterogeneous global model has been adopted in previous works taking into account the diffusion inside the chip (for example, Gustafson, Shelder, McKean, & Finlayson, 1983; Jiménez, Gustafson, & McKean, 1989; Agarwal, 1993).

This kinetics implies a number of concentrations as state variables that include six organic compounds in the solid matrix

- high and low reactivity lignin,
- high and low reactivity hemicellulose,
- high and low reactivity cellulose.

under the effect of two inorganic reactants

- sodium hydroxide;
- sodium sulfide.

This gives rise to 22 state equations (8 for the free liquid, 8 for the entrapped liquid and 6 for the solid matrix). In spite of this somewhat large number of state variables, the model of Mirams and Nguyen (1996) was chosen because it presents a dependency of the delignification rate on the hydroxide ion concentration, in opposition to other kinetic models where the delignification rate is in a given period of time independent of the hydroxide ion concentration thus leading to reaction (and, therefore, to consumption of hydroxide ion) even before this inorganic species is present inside the wood chips. This would lead to negative concentrations, which is physically meaningless.

The results presented here were obtained by discretizing the half-thickness of the chip in 10 intervals, i.e., $n = 10$.

The operating conditions used in this simulation study are as follows:

- the temperature starts at 100°C and increases linearly for 1 h until it reaches 160°C, being constant thereafter,
- the liquid (including both free and entrapped) to wood ratio is approximately $6.13 \text{ dm}^3 \text{ kg}^{-1}$,
- both Q_{in} and Q_{out} are set to zero,
- the initial free liquid concentration of hydroxide ion is 1.20 mol dm^{-3} and of hydro-sulfide ion is 0.18 mol dm^{-3} ,
- at time zero, the chips are fully impregnated with water,
- chips are 6 mm thick, 50 mm long and 35 mm wide.

The industrial purpose of the cooking is to decrease the amount of lignin in the solid structure of wood in order to release the cellulosic fibers, while preserving the chemical properties of their main components, i.e., cellulose and hemicellulose. For a given operating scenario, the tradeoff between high delignification and low carbohydrate attack determines the industrial reaction time. Simulations were performed to cover 250 min ($\approx 4.2 \text{ h}$), a typical cooking time.

The two inorganic chemicals in the free liquor are transferred to the chips and react with the six organic compounds of the solid matrix, dissolving them into the entrapped liquid. The chemical degradation and dissolution of the solid structure of the wood is responsible for the increase of the porosity of the chips. This has been ignored in previous attempts to describe the intra-particle process heterogeneity (Johnsson, 1970; Tyler, 1982; Gustafson et al., 1983; Gustafson, 1988; Agarwal, 1993; Agarwal, Gustafson, & Arasakesari, 1994; Agarwal & Gustafson, 1997; Li, Phoenix, & Macleod, 1997). In these works a considerable discrepancy between the experimental values and the predicted space averaged profiles does exist and the range of values anticipated for non-uniformity is far from reality. This inaccuracy subsists even when different parameters for different data sets are employed in the simulation (Gustafson et al., 1983; Agarwal, 1993; Agarwal et al., 1994; Agarwal & Gustafson, 1997). The thicker the chips, the more evident is the weakness of these models. Agarwal (1993) (see also Agarwal et al., 1994; Agarwal & Gustafson, 1997) tries to overcome the difficulties described in Gustafson et al. (1983) by introducing the concept of an “equivalent sphere” with the same specific surface area as the chip but the results, although better, are still unsatisfactory.

The porosity of the chips varies significantly during the cooking as it is portrayed in Fig. 3, where it is also possible to see that its evolution is different from point to point along the chip thickness, since it is the result of the local rates of the reactions involved.

Three of the six organic chemicals that form the solid matrix are very reactive. Their fast dissolution explains the

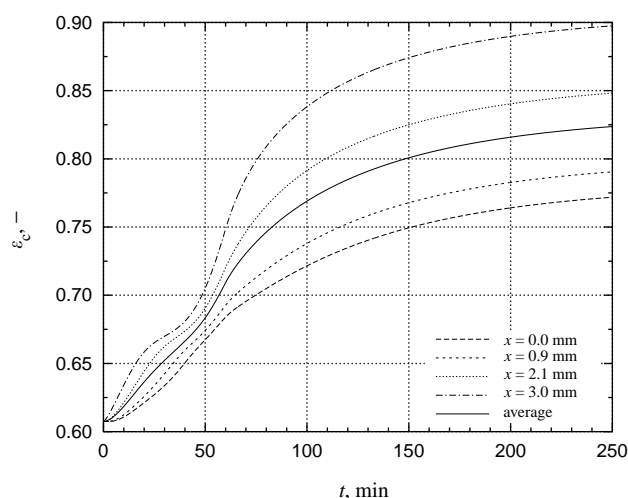


Fig. 3. Porosity profiles at different spatial positions in the wood particles.

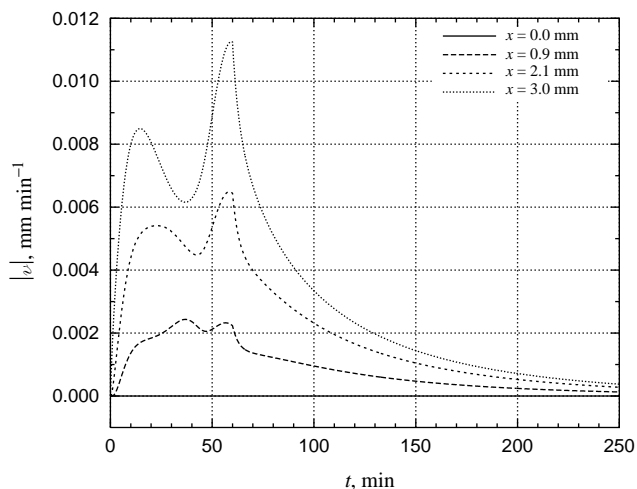


Fig. 4. Absolute values of interstitial velocity profiles inside the wood chips.

rapid increase of porosity seen at the chip surface in the beginning of the operation, despite the relatively low temperature. After this initial phase the porosity changes are attributable almost exclusively to the dissolution of the three less reactive organic components whose behavior, though, is strongly influenced by the progressive increase in the reactor temperature. At $t = 60 \text{ min}$, the time derivative of the porosity starts to diminish, due to the progressive lowering of concentrations in wood and of the inorganic reactants.

As a result of the porosity evolution highlighted in Fig. 3, the wood particles soak free liquid to fill up the dissolved volume of solid matrix, giving rise to an inward flow of liquid. The absolute values of the velocity profiles associated to such a flow are presented in Fig. 4 for several chip positions.

The absolute value of the velocity attains its maximum once the highest temperature is reached ($t = 1 \text{ h}$).

Thereafter, although the temperature remains high and constant, the reaction rates decrease gradually because of the strong consumption of reactants and, therefore, the absolute value of the velocity also diminishes. The two peaks exhibited by the velocity profiles correspond to the quickest changes in porosity caused by the chemical destruction of the wood: the first is associated with the high-reactivity components and the second with those of low-reactivity together with the high reacting temperatures. The fact that the porosity is a monotonous increasing function along time stresses the first peak in detriment of the second, since a smaller porosity leads to a smaller interstitial area available for the liquid flow (see Eq. (15)). It can also be seen that the module of the velocity, at a certain time, always decreases from the external surface (dotted line) to the center of the chip (solid line). This means that the increase of the interstitial area (bigger in the outer zones of the particle) plays a less significant role on the velocity than the spatial cumulative changes of porosity from the chip center up to the point under consideration.

An interesting comparison that can be made is between the convective flux associated to this intra-particle velocity and the total (convective and diffusive) flux. The average ratio between the convective and the total fluxes for the species OH^- (the most important reactant that is transferred into the chip) is, in this example, approximately 0.0865. This reinforces the idea that convection (representing 8.65% of the total transport) should be taken into account. However, it also should be noted that the results presented here are merely illustrative and do not intend to be quantitatively precise.

The inorganic reactants, initially present in the free liquid only, gradually move into the chips. This transfer, due to both diffusion and convection transport mechanisms, promotes concentration profiles along the chip thickness as illustrated in Fig. 5 for the concentration of the hydroxide ion.

This variable has a determining effect on the degradation and dissolution of the wood components. Therefore, uneven concentration profiles of this inorganic species have a strong and negative effect upon the desirable uniformity of the pulp. An interesting fact pointed out in Fig. 5 is that the central parts of the chip are never exposed to as much aggressive chemical conditions as those verified in the outer parts. In fact, while the hydroxide concentration at the chip center is always below 0.1 mol dm^{-3} , at the chip edge it can reach more than 0.6 mol dm^{-3} . As expected, the spatial concentration gradients of the inorganic reactants are higher for relatively short cooking times, when the free liquid is still very rich in these species. Later, their profiles tend to flatten out, as a consequence of the transport phenomena, with very low concentration values due to their consumption by the chemical reactions.

To highlight the effect of the intra-particle convection that is caused by changes in chip porosity, a simulation run was performed where this morphological property of the chip was deliberately kept constant. Such a procedure forces the

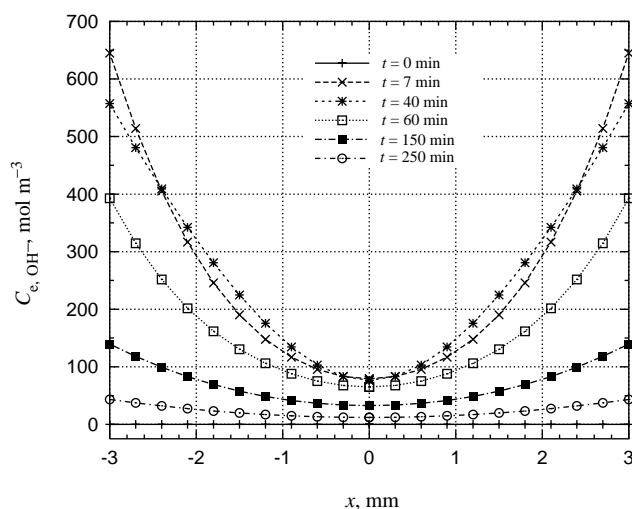


Fig. 5. Concentration profiles of OH^- along the spatial particle coordinate ($C_{f,\text{OH}^-}|_{t=0} = 1200 \text{ mol m}^{-3}$).

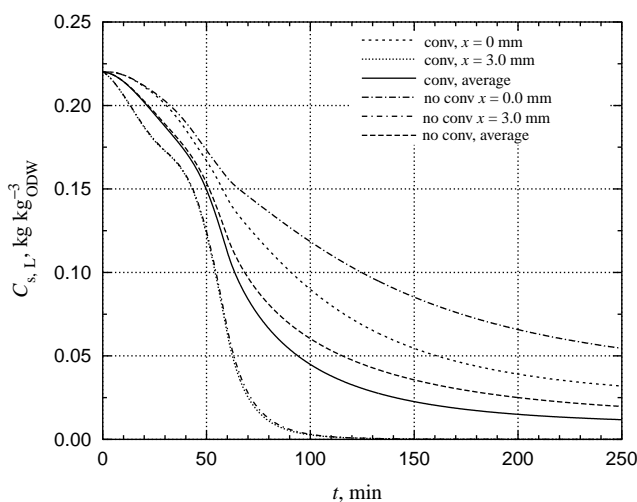


Fig. 6. Solid matrix lignin profiles with and without convection.

intra-particle velocity to remain equal to zero throughout the whole pulping process and, therefore, it cancels the convective term in the model equations while maintaining all other features. In such a particular situation, the resulting model equations are exactly those used by Gustafson et al. (1983) with the exception of the kinetic model. The lignin profiles in the solid matrix that result from this run are plotted in Fig. 6, together with those corresponding to the case where the intra-particle convection is considered.

Although both models predict similar profiles for the chip edge concentration of lignin in the solid matrix, there is a substantial difference between the corresponding predictions for the chip center. In terms of spatial average values (solid and dashed lines), this maximum difference is softened but it is very clear. The model that does not consider intra-particle convection overestimates the average solid matrix lignin

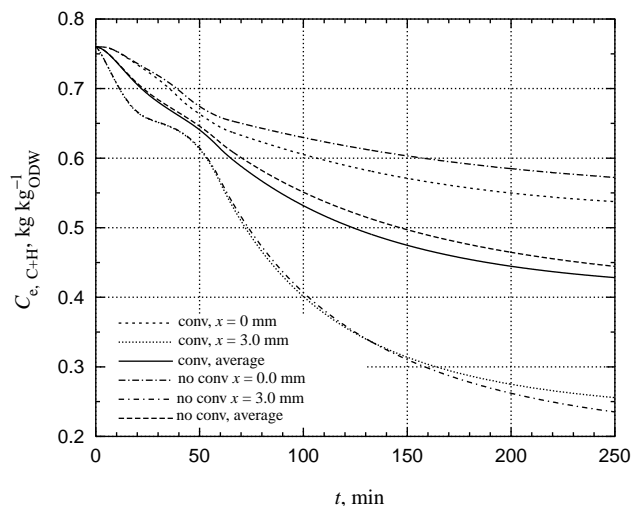


Fig. 7. Solid matrix carbohydrates profiles with and without convection.

concentration and above all the particle non-uniformity, relatively to the model proposed here. The discrepancy between the two averaged values begins at $t \approx 50$ min, has a maximum at $t \approx 100$ – 150 min and decreases slightly at the end of the operation. This mismatch is remarkably coincident with that verified between the diffusion model used by Gustafson et al. (1983) and the data used in its validation. This anticipates a strong predictive potential for the model with intra-particle convection. As it has been pointed out above, the results presented in this paper are qualitative and have demonstrative purposes only. Quantitative results require a convenient choice of parameters, namely of the diffusion coefficients (now functions of the porosity only).

The concentration profiles of the carbohydrates in the wood predicted by the two models can be seen in Fig. 7. Once more the model taking into account the intra-particle mass transport by convection forecasts less inhomogeneity than that where this phenomenon is ignored. The considerable disparity between the average values in Fig. 7 again suggests that the correcting key for the inability of the 1-D slab model to reproduce the experimental data lies on the accounting of the important porosity changes and the consequent intra-particle convection transport mechanism.

Finally, Fig. 8 reveals the differences between the predictions of the two models under analysis in what concerns the yield of the pulping process. The profiles along the chip thickness, especially those corresponding to the end of the cooking, corroborate the overestimation of pulp non-uniformity by the diffusion model relatively to that proposed here that accounts for both diffusion and intra-particle convection.

4. Conclusions

Although several authors have been studying the effect of intra-particle convection on the behavior of heterogeneous

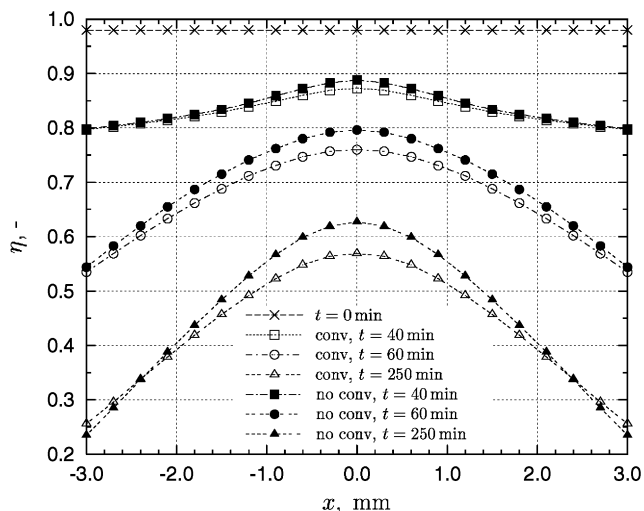


Fig. 8. Yield predictions with and without convection.

systems, none until now has addressed this problem when it is caused by chemical reaction of the particles structure. Usually, these are seen as inert materials where the catalyst is supported and the convection origin lies on the fact that there is a pressure drop along the reactor, that leads to a constant intra-particle velocity. Here, a wider methodology is taken, with a time and space variable velocity, since it depends on time and spatial evolutions of the reaction rates. The approaches for intra-particle convection developed until now are not suitable for the case of variable porosity of the particles. The modeling approach adopted here was applied to the heterogeneous process of kraft pulping of wood. The inclusion of convection induced by the increase of the chip porosity enables a more realistic and potentially accurate description of this process. Such a tool is important at a industrial level because it can be used to achieve higher production rates and pulp of higher quality. In spite of the preliminary nature of the values used for the mass transfer coefficients across the film and the diffusion coefficients (now simple functions of the chip porosity), the model exhibits promising features in overcoming significant prediction inaccuracies of previous investigations where the diffusion is the only transport mechanism that is accounted for. The model developed here provides a better understanding of the heterogeneous nature of the cooking process and is a step ahead towards the effective control of the undesirable non-uniformity of the pulp.

Notation

a_c	superficial area of all the chips, m^2
a_{fe}	total area of interface between free and entrapped liquids, m^2
$C_{p,k}$	mass concentration of the species k in the flow or phase p (with $p = in, f, e$), $kg\ m^{-3}$

$C_{s,k}$	mass fraction of the species k in the solid phase based on oven dry wood, dimensionless
\mathcal{D}_k	effective diffusion coefficient for species k , $\text{m}^2 \text{s}^{-1}$
$\mathcal{D}_{m,k}$	molecular diffusivity for species k , $\text{m}^2 \text{s}^{-1}$
$\mathcal{D}'_{m,k}$	ratio between the molecular diffusivity for species k and the tortuosity, $\text{m}^2 \text{s}^{-1}$
K_k	mass transfer coefficient for the species k , m s^{-1}
L	particle thickness, m
n	number of discretization intervals along x , dimensionless
n_e	number of equations for the entrapped liquid at each chip position, dimensionless
n_{eq}	total number of ODEs which constitute the discretized model, dimensionless
n_f	number of equations for the free liquid, dimensionless
n_i	number of inorganic species, dimensionless
n_o	number of organic species, dimensionless
n_s	number of equations for the solid phase at each chip position, dimensionless
Q	flow of liquid at a generic point inside the chip relatively to x axes, $\text{m}^3 \text{s}^{-1}$
Q_{fe}	flow from free to entrapped phase, $\text{m}^3 \text{s}^{-1}$
Q_{in}	inlet flow in the reactor, $\text{m}^3 \text{s}^{-1}$
Q_{out}	outlet flow from the reactor, $\text{m}^3 \text{s}^{-1}$
Q	intra-particle flow of liquid at a generic x point of the chip, $\text{m}^3 \text{s}^{-1}$
\mathcal{R}_k	reaction rate for species k , $\text{kg kg}_{ODW}^{-1} \text{s}^{-1}$
t	time, s
v	intra-particle velocity, m s^{-1}
V_f	volume of free liquid, m^3
x	spatial coordinate along the thickness of the chip, m

Greek letters

ε_c	chip porosity, dimensionless
$\varepsilon_{c,i}$	initial chip porosity, dimensionless
η	yield, dimensionless
$\rho_{c,OD}$	specific mass of an oven dry chip, kg m^{-3}
τ	tortuosity factor, dimensionless

Acknowledgements

Financial support granted by Ministry of Science and Technology under Project Praxis 3/3.2/PAPEL/2327/95 is gratefully acknowledged. The first author also wishes to thank Program Praxis for her scholarship PRAXIS/4/4.1/BD/3338.

References

- Agarwal, N. (1993). *Modeling of continuous pulping*. Ph.D. thesis, University of Washington.
- Agarwal, N., & Gustafson, R. (1997). A contribution to the modeling of kraft pulping. *The Canadian Journal of Chemical Engineering*, 75(2), 8–15.
- Agarwal, N., Gustafson, R., & Arasakesari, S. (1994). Modeling the effect of chip size in kraft pulping. *Paperi ja Puu*, 76(6–7), 410–416.
- Aris, R., & Kehoe, J. P. G. (1973). Communications on the theory of diffusion and reaction-IX. Internal pressure and forced flow for reactions with volume change. *Chemical Engineering Science*, 28, 2094–2098.
- Brown, P. N., Hindmarsh, A. C., & Petzold, L. (1998). Consistent initial condition calculation for differential-algebraic systems. *SIAM Journal of Science Computing*, 19, 1495–1512.
- Brown, P. N., Hindmarsh, A. C., & Petzold, L. R. (1994). Using Krylov methods in the solution of large-scale differential-algebraic systems. *SIAM Journal of Science Computing*, 15, 1467–1488.
- Costa, I. M. M., Francisco, S. C. P., Simão, J. P. F., Egas, A. P., & Castro, J. A. A. M. (2001). The nature of mass transfer of alkali to wood chips during kraft pulping. In *CHEMPOR'2001*, Aveiro, Portugal, in press.
- Fernandes, N. C. P., & Castro, J. A. A. M. (2000). Steady-state simulation of a continuous moving bed reactor in the pulp and paper industry. *Chemical Engineering Science*, 55(18), 3729–3738.
- Ferreira, R. M. Q. (1988). *Contribuição para o estudo de reatores catalíticos de leito fixo: Efeito da convecção em catalisadores de poros largos e casos de catalisadores bidispersos*. Ph.D. thesis, Universidade do Porto.
- Ferreira, R. M. Q., Costa, A. C. A., & Rodrigues, A. E. (1996). Effect of intraparticle convection on the transient behavior of fixed-bed reactors: Finite differences and collocation methods for solving unidimensional models. *Computers and Chemical Engineering*, 20(10), 1201–1225.
- Froment, G. F., & Bischoff, K. B. (1990). *Chemical reactor analysis and design* (2nd ed.). New York: Wiley.
- Gustafson, R. R. (1988). The role of diffusion during initial delignification of alkaline pulping. *Tappi Journal*, 71(4), 145–147.
- Gustafson, R. R., Shelder, C. A., McKean, W. T., & Finlayson, B. A. (1983). Theoretical model of the kraft pulping process. *Industrial and Engineering Chemistry, Processing Design and Development*, 22(1), 87–96.
- Jiménez, G., Gustafson, R. R., & McKean, W. T. (1989). Modelling incomplete penetration of kraft pulping liquor. *Journal of Pulp and Paper Science*, 15(3), J110–J115.
- Johnsson, L. (1970). *Mathematical models of the kraft cooking process*. Technical report 11, Department of Control Engineering, Chalmers University of Technology, Gothenburg, Sweden.
- Komiyama, H., & Inoue, H. (1974). Effects of intraparticle flow on catalytic reactions. *Journal of Chemical Engineering of Japan*, 7(4), 281–286.
- Leitão, A., & Rodrigues, A. E. (1996). Modeling of biodegradation/adsorption combined process in fixed-bed biofilm reactors: Effects of the intraparticle convection flow. *Chemical Engineering Science*, 51(20), 4595–4604.
- Li, S., & Petzold, L. R. (1999). *Design of new DASP for sensitivity analysis*. Technical report TRCS99-28, University of California at Santa Barbara.
- Li, J., Phoenix, A., & Macleod, J. M. (1997). Diffusion of lignin macromolecules within the fibre walls of kraft pulp. Part I: Determination of the diffusion coefficient under alkaline conditions. *The Canadian Journal of Chemical Engineering*, 75(2), 16–22.
- Lopes, J. C. B., Dias, M. M., Mata, V. G., & Rodrigues, A. E. (1995). Flow field and non-isothermal effects on diffusion, convection and reaction in permeable catalysts. *Industrial and Engineering Chemistry Research*, 34(1), 148–157.
- Mirams, S., & Nguyen, K. L. (1996). Kinetics of kraft pulping of *Eucalyptus globulus*. *AIChE Symposium Series*, 92(311), 1–9.
- Nan, H. S., Dias, M. M., Lopes, J. C. B., & Rodrigues, A. E. (1996). Diffusion, convection and reaction in catalyst particles: Analogy between slab and cylinder geometries. *The Chemical Engineering Journal*, 61, 113–122.

- Nir, A., & Pismen, L. M. (1977). Simultaneous intraparticle forced convection, diffusion and reaction in a porous catalyst. *Chemical Engineering Science*, 32, 35–41.
- Pfeiffer, J. F., Chen, J. C., & Hsu, J. T. (1996). Permeability of gigaporous particles. *A.I.Ch.E. Journal*, 42(4), 932–936.
- Pismen, L. M. (1976). Convective currents induced by chemical reactions in partially-filled porous media. *Chemical Engineering Science*, 31, 693–699.
- Sun, W., Costa, A. V., & Rodrigues, A. E. (1995). Determination of effective diffusivities and convective coefficients of pure gases in single pellets. *The Chemical Engineering Journal*, 57, 285–294.
- Tyler, D. B. (1982). Predicting rejects from kraft cooking of overthick chips. *Svensk Papperstidning*, 85(18), R180–R184.